Wavelength tunable and broadband variable fiber-optic attenuators using liquid crystals

Khan, Sajjad, Riza, Nabeel

Sajjad A. Khan, Nabeel A. Riza, "Wavelength tunable and broadband variable fiber-optic attenuators using liquid crystals," Proc. SPIE 5814, Enabling Photonics Technologies for Defense, Security, and Aerospace Applications, (24 May 2005); doi: 10.1117/12.604910

SPIE.

Event: Defense and Security, 2005, Orlando, Florida, United States

Wavelength Tunable and Broadband Variable Fiber-Optic Attenuators using Liquid Crystals

Sajjad A. Khan and Nabeel A. Riza
Photonic Information Processing Systems Laboratory
College of Optics & Photonics/(CREOL)
University of Central Florida, 4000 Central Florida Blvd., Orlando, FL 32816-2700
Tel: 407-823-6829; Fax: 407-823-6880; E-mail: nriza@mail.ucf.edu

ABSTRACT

Fiber-Optic Variable Optical Attenuators (VOAs) are demonstrated using Liquid Crystals (LC) for broadband as well as wavelength tunable applications. Attenuation is achieved by using a beam spoiling approach implemented via electrically reconfigurable non-pixelated no moving parts Nematic LC deflectors. The VOAs feature in-line architecture and polarization insensitive design without the use of bulky polarization splitting and combining optics. The proof-of-concept VOAs in the 1550 nm band demonstrate >30 dB attenuation ranges, low polarization dependent losses and low power consumption. Applications for these VOAs include agile wavelength tunable secure data communications networks and RF sensor systems.

Introduction

As the demand for high data rate telecommunication networks increases, optical devices are sought that are low in cost, utilize little drive power, and have broadband robust operation. The Variable Optical Attenuator (VOA) is one such component that is needed in wavelength division multiplexed (WDM) systems to dynamically control the channel power per wavelength. The fiber-optic VOA is a basic processing element in many optical systems. It is desirable that such a VOA is controlled with minimal electrical power and operates over broad optical bands. A variety of technologies have been proposed to realize single channel VOAs such as micro-mirrors[1], acousto-optics[2], and thermo-optics[3,4]. Liquid crystals (LCs), because of their no moving parts, low loss, and low power consumption nature have long been considered an excellent alternative for making optical components.[5] Specifically analog operation [6-8] and all-digital operation LC VOAs [9,10] have also been proposed. An issue with polarization controlled LC VOAs is their need to use bulky polarization beam displacement and combining optics such as crystal beam displacement prisms (BDPs) to enable polarization independent designs. In addition, these VOAs are extremely sensitive to polarization extinction changes such as due to temperature swings in the LC cells that in-turn lead to unwanted VOA light throughput fluctuations. In effect, any deterioration in LC cell polarization extinction ratios causes useful signal light to be rejected via the combining BDP. Thus, an LC VOA that can counter this excess loss variation problem would be highly desirable.

In this paper, we show a simple LC VOA structure that forms a compact VOA which does not use BDPs and moreover can eliminate the extinction ratio-based loss throughput problem.[11-12] Specifically, this VOA design implements attenuation via the

Enabling Photonics Technologies for Defense, Security, and Aerospace Applications,
edited by A. R. Pirich, M. J. Hayduk, E. J. Donkor, P. J. Delfyett, Jr., Proc. of SPIE Vol. 5814
(SPIE, Bellingham, WA, 2005) · 0277-786X/05/$15 · doi: 10.1117/12.604910

use of LC-based optical beam spoiling. The ref. 12 VOA can operate over a broad optical band making it an essentially wavelength insensitive module. Yet, there are some applications where it is desirable to have a wavelength tunable VOA. Such applications include an optical receiver that requires the ability to tune to a chosen wavelength in a broad optical band and simultaneously has the feature of controlling optical light flow or attenuation in the photo-detection optoelectronics. In other words, an electronically tunable wavelength sensitive VOA is required. Another possible application is a gain controlled tunable optical transmitter. In this paper, we also show how the ref. 12 VOA can be simply modified to realize the desired wavelength agile VOA.[13] Earlier proposed was a hybrid LC plus mirror optics approach to free-space beam controls within fiber-optic structures where the excellent fine pointing ability of LC optics is exploited for super-fine free-space beamforming and the much better (compared to LCs) larger angular range of mirror optics is engaged to implement the high angular dynamic range beam pointing.[11] Shown in this paper is how the hybrid LC-mirror beam controls approach is combined with wavelength sensitive optics within the ref. 11 VOA design to realize the desired wavelength agile VOA. Independently, micro-electromechanical systems (MEMS) mirror optics alone has been engaged to realize single wavelength selection modules for applications such as wavelength scanned optical spectrum analysis and agile wavelength selection for an optical receiver.[14,15] The rest of the paper describes the designs and demonstrations of fiber-optic VOAs using a non-pixelated NLC deflector device to implement beam spoiling and wavelength selectivity in a no moving parts-implementation.

LC-Deflector Based VOA Theory

Figure 1(a) shows one in-line design of the proposed Nematic Liquid Crystal (NLC) deflector-based VOA using self-imaged identical fiber Gradient Index (GRIN) rod lenses.[16-17] The two GRIN lenses are separated by 2d, where d is the beam waist location distance leading to a low loss design. Two NLC deflectors with orthogonal NLC directors are placed between the GRIN lenses. Figure 1(b) shows the second approach to realize the VOA using a dual fiber collimator, a single NLC deflector, and a 45^{o} power Faraday rotator-mirror pair. This reflective design results in a more compact architecture as compared to that of Figure 1(a). Finally, Fig. 1(c) shows the third proposed in-line VOA design that takes advantage of today's highly low loss (e.g., <1 dB) compact optical circulator devices. In the absence of any NLC device control signal, all input light is directed to the desired VOA output port. For VOA control, the amplitude and frequency of the NLC deflector electrical drive signals are varied to implement beam deflections leading to the desired VOA attenuation level. The NLC deflector is different from an ordinary parallel rub NLC cell in that instead of having the NLC layer sandwiched between two Indium Tin Oxide (ITO) electrodes, the NLC material is sandwiched between an ITO electrode which acts as the ground electrode, and a high impedance control electrode (see figure 2(a)). Earlier, the use of a high resistance layer with two parallel electrical contacts was proposed to generate a smooth voltage ramp between these contacts to form a pixel-free deflector.[18-19] At the edges of the control electrode, linear electrical contacts are deposited which are used to apply the drive signal. When a signal is applied to one of these linear electrical contacts, the voltage drops

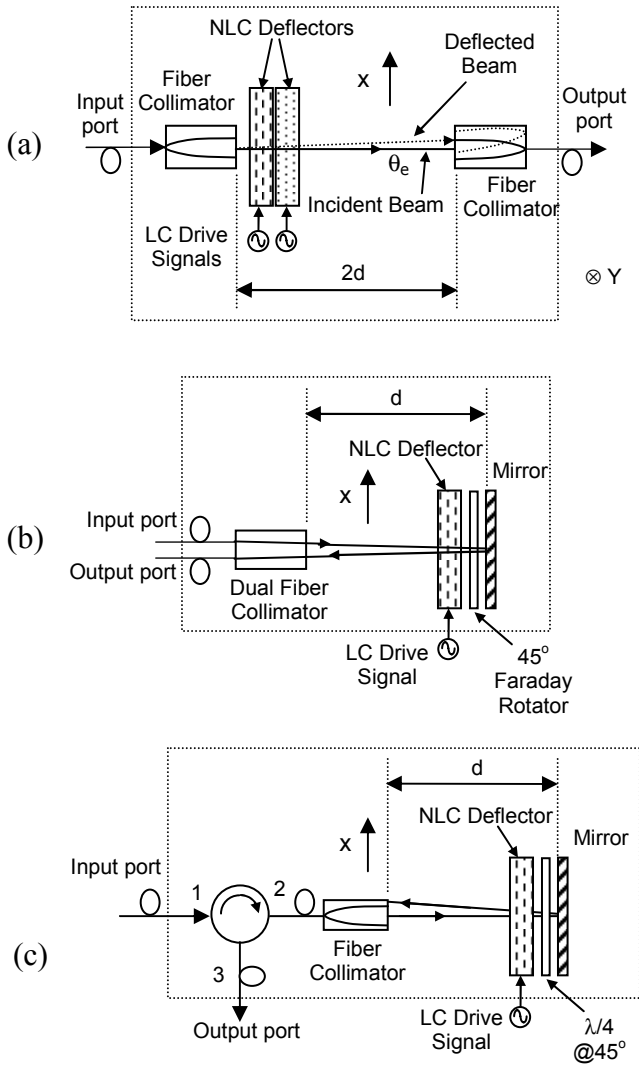

Fig. 1. Top views of proposed NLC beam-spoiling VOA designs using (a) two fiber collimators and two NLC deflectors with orthogonal NLC directors, (b) a dual collimator and a single NLC deflector with 45° Faraday rotator-mirror pair, and (c) an optical circulator, single fiber collimator with a single NLC deflector and 45° Faraday rotator-mirror pair. λ/4: Quarter wave plate.

linearly across the high impedance layer. The resulting E-field present across the NLC layer varies linearly across the aperture of the device leading to an index modulation that varies across the aperture of the device in a near-linear fashion (see Figure 2(b)). Notice that this index modulation is along the NLC director and thus can be seen only by that component of the input polarized light which is along the NLC director. As a consequence, a scheme is needed to cater for both orthogonal polarization components of the input light entering via the VOA fiber-optics. In Figure 1(b, c), the 45° power Faraday rotator (or a quarter wave plate) with a mirror makes the reflective VOA design polarization insensitive. For the transmissive Figure 1(a) design, two orthogonal director NLC deflectors cater for both the components of the input polarization, making a

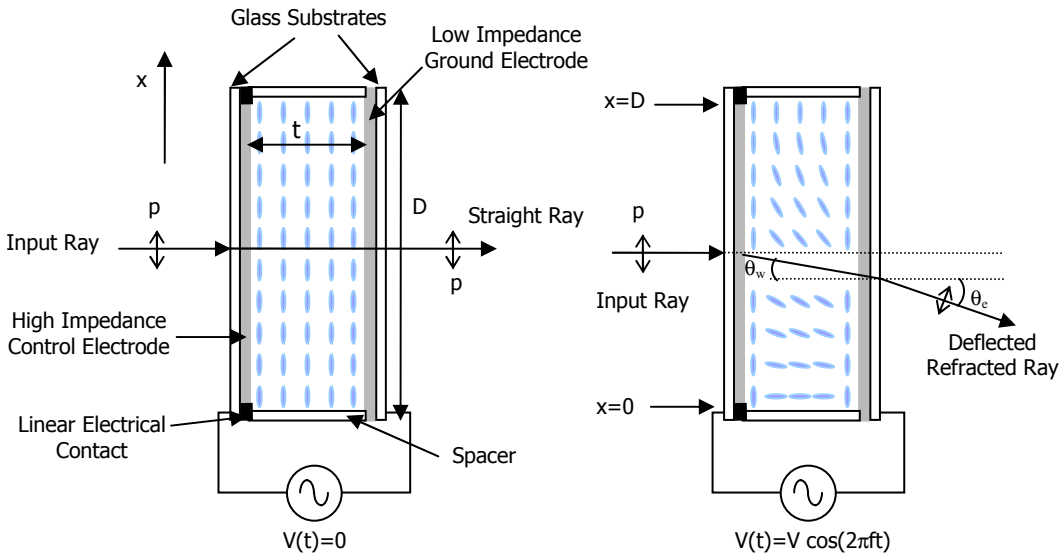

(a) (b)

Fig. 2. Top views of the NLC deflector used to realize the VOAs. NLC molecule orientations are shown for (a) zero control signal applied and (b) when a control signal is present that reorients the NLC molecules to induce a spatial wedgelike refractive index change. *p*: horizontally polarized light component.

polarization independent VOA. Thus a thin optical wedge formed in the NLC layer results in the refraction of the laser beam away from its original path, causing it to deflect along one dimension and hence un-optimize light coupling with the receiving GRIN lens.

Specifically in Figure 1(a), one orthogonal polarization component deflects in the x-direction while the other orthogonal polarization component deflects in the y-direction. This is because the NLC deflectors used are identical design devices, except being physically flipped by 90^o with respect to each other for alignment purposes. This can be overcome by having two NLC cells with orthogonal directors but with the linear metallic electrical contacts parallel in both the cells such that the resulting phase ramp and hence the beam deflection for both the polarizations is in the same direction. Because of the symmetry of the VOA design, attenuation levels due to beam spoiling of both polarizations is the same, leading to a polarization insensitive design. Nevertheless, note that since two NLC deflectors are used with possible independent drive signals, any non-uniformity due to fabrication of the two cells can be cancelled by using two calibrated and independent drive signals for the two cells. For the Figure 1(b, c) designs, both polarizations undergo 1-D deflections in the x direction and so using a single NLC deflector is sufficient to deliver the polarization independent VOA operation. Next, the theoretical foundations are laid for the proposed NLC deflector-based VOA.

With reference to Figure 2, a ray polarized along the molecular NLC director passing through the NLC deflector device acquires a phase shift at the device position x that can be expressed as:

$$\phi(V, f, x) = [2\pi/\lambda]\, n(V, f, x)\, t \qquad (1)$$

where λ is the optical wavelength, t is the NLC layer thickness, n(V, f, x) is the electrically controlled NLC refractive index the light sees, and V is the amplitude in Volts and f is the frequency in Hertz of the NLC device drive signal. Looking at the two extreme ray positions of x=0 and x=D, the beam deflection of the entire wavefront incident on the NLC deflector can be studied. Specifically, the x=0 position ray suffers a phase shift given by:

$$\phi(V, f, x=0) = \phi_o = [2\pi/\lambda]\, n(V, f, 0)\, t\,, \qquad (2)$$

while the extreme ray at x=D suffers a phase shift given by:

$$\phi(V, f, x=D) = \phi_D = [2\pi/\lambda]\, n(V, f, D)\, t\,. \qquad (3)$$

Hence the phase shift between the edges of refracted plane wave exiting the NLC deflector is given by:

$$\Delta\phi = \phi_D - \phi_o\,, \qquad (4)$$

where between the x=0 and x=D points, the incident plane wave acquires a linearly increasing phase shift. At x=D, the applied voltage is designed via the electrode structure to be zero, so the index seen by the incoming ray of p-polarization is essentially n_e, the NLC material extraordinary index of refraction. Therefore $\phi_D = 2\pi/\lambda\ (n_e\ t)$ and $\Delta\phi$ becomes:

$$\Delta\phi = (2\pi/\lambda)\, [n_e - n(V, f, 0)]\, t\,. \qquad (5)$$

Similarly, note that at the x=0 location where the other device electrode is present, V and f can be controlled to set $n(V, f, x=0) = n_o$, where n_o is the ordinary refractive index of the NLC material. In this case, the NLC deflector is generating its maximum birefringence $\Delta n = n_e - n_o$ and hence also produces the largest phase shift between rays across the device aperture D. This in turn leads to the maximum beam deflection angle θ_m for the programmable NLC deflector. From phased array theory, the beam steered angle θ_w due to an inter-element phase shift $\Delta\phi$ is given by:

$$(2\pi D/\lambda)\, \sin\theta_w = \Delta\phi, \qquad (6)$$

where D is the phased array inter-element distance or in this case the NLC device aperture. By equating equations (5) and (6), the electrically controlled deflector angle θ_w as seen by a wave polarized along the molecular director is written as:

$$(2\pi D/\lambda)\, \sin\theta_w = (2\pi/\lambda)\, [n_e - n(V, f)]\, t \qquad (7)$$

This in turn leads to:

$$\theta_w(V, f) = \sin^{-1}\, \{\frac{t}{D}\, [n_e - n(V, f)]\}, \qquad (8)$$

A laser beam passing through the described thin NLC deflector (see Figure 2) is refracted at the freespace output of the deflector by an angle θ_e that depends upon the average index <n> of the NLC material, and the electrically set deflector angle θ_w, and the index of the output media (in this case, air), leading to the expression:

$$<n>\, \sin\theta_w = \sin\theta_e\,. \qquad (9)$$

For a parallel rub NLC cell, <n> is given as:[20]

$$<n^2> = (n_e^2 + 2n_o^2)/3. \qquad (10)$$

Hence θ_e can be written as:

$$\theta_e = \sin^{-1}(<n>\, \sin\theta_w). \qquad (11)$$

It is because of the adjustable deflection angle θ_e in the air that the laser beam going back into the fiber collimator is displaced from its perfectly aligned self-imaging state, leading

to the controlled attenuation of light passing through the VOA. In addition, the output power coupled back into the fiber depends upon the separation distance between the NLC deflector and the fiber collimator. The deflected beam causes angular tilt and offset misalignments for the GRIN lens which result in a fiber-optic coupling loss.[16,17] For example, in the case of Figure 1(b) and (c) VOA designs, the attenuation offset misalignment x_o via beam deflection is given as:

$$x_o = d \tan\theta_e \tag{12}$$

Therefore, x_o becomes:

$$x_o = d \tan\{\sin^{-1}(<n> \sin\theta_w)\}, \tag{13}$$

and using the expression for θ_w from (8) gives:

$$x_0 = d \tan\left[\sin^{-1}\left[< n > \left\{\frac{t}{D}[n_e - n(V, f)]\right\}\right]\right]. \tag{14}$$

As the NLC deflector angles are designed to be small (e.g., $<0.21^o$), the small angle approximation of $\sin\theta \cong \tan\theta \cong \theta$ can be applied giving:

$$x_o \cong d < n > \left\{t/D\left[n_e - n(V, f)\right]\right\} = d < n > \theta_w . \tag{15}$$

In conclusion, the proposed VOA attenuation is controlled by producing a given beam offset misalignment x_o induced by an NLC deflector produced beam tilt misalignment angle θ_w. More specifically, it can be seen from equation (15) that the VOA attenuation depends upon the beam waist position d from the GRIN lens, the average NLC refractive index <n>, the NLC cell thickness t, device aperture D, device programmable birefringence n_e-n(V, f), and the drive signal voltage V and frequency f.

LC-Deflector Based VOA Experiment

The Figure 1(c) design is used as the proof-of-concept experimental setup at λ=1550nm for the proposed VOA. This design uses a 9 μm core single mode fiber (SMF) coupled collimator, an NLC deflector, a quarter wave plate (QWP) for 1550nm, a mirror and a circulator. The circulator and the single fiber collimator emulate the presence of a dual fiber collimator, as in Figure 1(b). First, the GRIN lens is characterized using the self-imaging technique.[16] The GRIN lens has a 5 mm physical diameter with a 2.5 mm exit beam $1/e^2$ diameter. Insertion loss for the GRIN lens using freespace-to-fiber coupling via the self-imaging mechanism is measured to be 0.4 dB. The beam waist location distance d of the chosen GRIN lens is 25 cm and the $1/e^2$ beam diameter is 2.49 mm. The QWP positioned within 1 mm of the mirror is oriented at 45^o with respect to the NLC director. The distance between the NLC deflector and the QWP is 13 mm. The insertion loss measured in this arrangement is 2.5 dB which includes a 0.7 dB loss per pass through the non-AR coated NLC deflector, a 0.4 dB free-space to GRIN lens coupling loss and 0.7 dB circulator loss. The NLC deflector used in the experiment has a clear aperture diameter D of 5 mm and a NLC layer with a uniform thickness t of 50 μm. The NLC used is Merck BL006 that has a manufacturer specified birefringence ($\Delta n = n_e - n_o$=1.816-1.53) of 0.286 at 25^oC room temperature and λ=589.3 nm.[21] The NLC birefringence Δn

depends upon the operating wavelength. Typically for NLCs with large birefringence (e.g. $\Delta n \sim 0.2$) in the visible band such as the Merck BL006, the birefringence decreases by ~15-20% going from visible to near infrared band.[22-23] The birefringence was also measured at 1550 nm and 25°C to be 0.229, which is within the 15-20% approximation range. Hence, for a given device drive signal, the VOA attenuation will decrease for longer wavelengths as compared to that for the shorter wavelengths. For example, VOA operation in the 35nm bandwidth C telecommunications band centered at 1545 nm is relatively constant due to small expected birefringence variation (typically <1%) within this infrared wavelength region[22]. Using equation (10), the average refractive index <n> is then calculated to be 1.63. Using the mentioned NLC deflector specifications and equation (8), the deflector angle θ_w maximum obtained using this device at 1550 nm is 2.29 mradian (0.131°). As listed in Table 1, the maximum angle θ_e at which the laser beam emerges from the NLC deflector is calculated using equation (11) to be 3.73 mradian (0.21°). Table 1 also gives the expected VOA beam angular and lateral misalignments for a variety of design specifications including the present experimental design. It can be concluded from Table 1 that using a given NLC device with a smaller aperture and hence larger beam deflection angle will result in a compact VOA design.
Figure 3(a) shows the measured VOA optical attenuation for the Figure 1(c) VOA as a function of the drive signal frequency f using a V= 5 Volt square wave signal. Figure 3(b) shows the measured optical attenuation as a function of the applied square-wave voltage for an f=2.7 kHz signal drive. The VOA attenuation dynamic range in both these cases is ~30 dB, generated by the combined tilt and offset beam spoiling effects. The PDL is measured to be <0.8 dB whereas the VOA resolution based on the resolution of present drive electronics is measured to be ±0.1 dB. Due to the large 5 mm aperture and large 50 μm thickness of the NLC layer, the response time of the current VOA is of the order of 1 second. The insertion loss and the response time can further be reduced by varying the parameters of the NLC deflector such as the thickness of the cell and its clear aperture. Note that because of the large "d" GRIN lens used in the experiment for ease of implementation, the NLC deflector and related retro-reflecting polarization independence creating optics are not in close proximity, thereby not negating PDL to the desired <0.2 dB. For a custom design, where the NLC deflector, QWP, and mirror are all stacked together with a short "d" dual collimator GRIN lens, both lower PDL and insertion loss can be achieved.

LC-Deflector Based Wavelength Tunable VOA

Figure 4 shows a hybrid design wavelength agile fiber-optic VOA. The basic design uses a fiber-optic circulator (C), a transmissive volume Bragg grating (VBG), one LC deflector, a quarter wave plate (QWP), and a mirror M. The design is similar to the Fig. 1(c) VOA design, except for the insertion of the grating optic and the active use of both the LC and mirror optics. The circulator is used to direct input and output light to and from the module. The input light is coupled to the freespace optics using a self-imaging type single mode fiber (SMF) gradient index (GRIN) rod lens.[16] A QWP is placed between the LC deflector and M to minimize polarization dependent loss (PDL) in the overall module. In addition, the QWP produces the desired linear polarization flipping

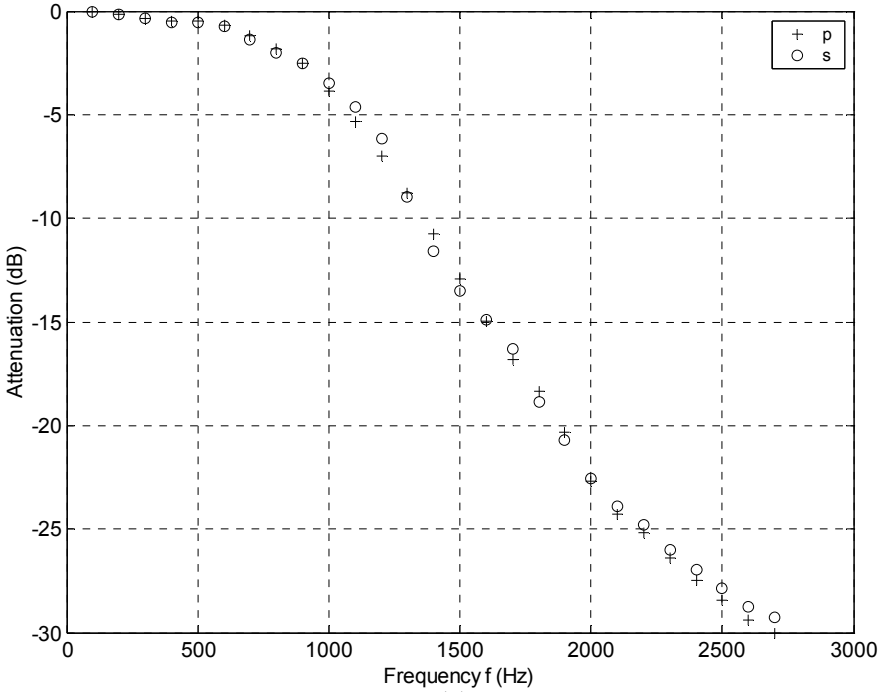

(a)

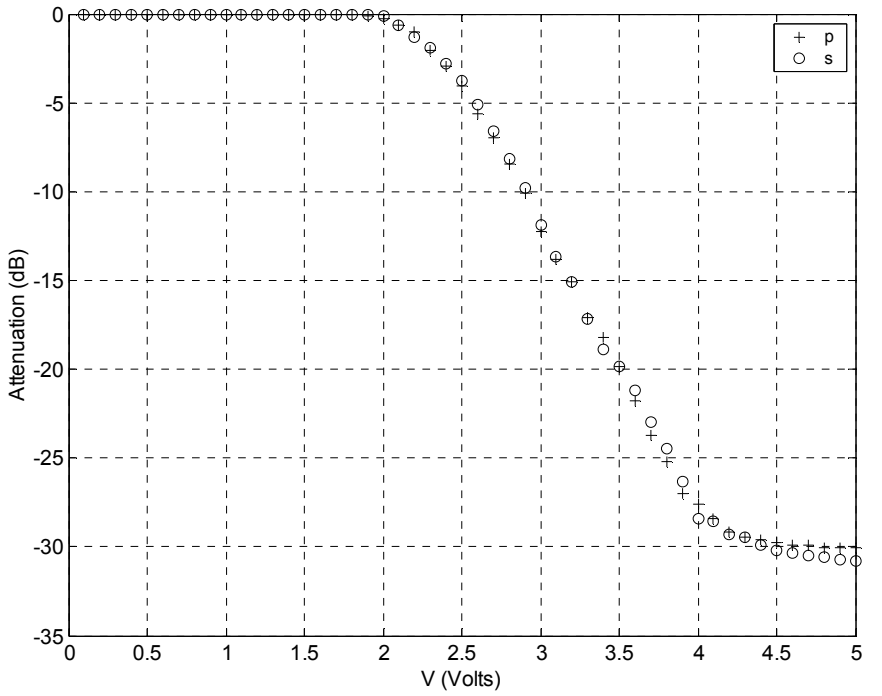

(b)

Fig. 3. Measured optical attenuation as a function of (a) drive frequency and (b) voltage. p: horizontally polarized light component parallel to cell nematic director. s: vertically polarized light component normal to the device NLC director.

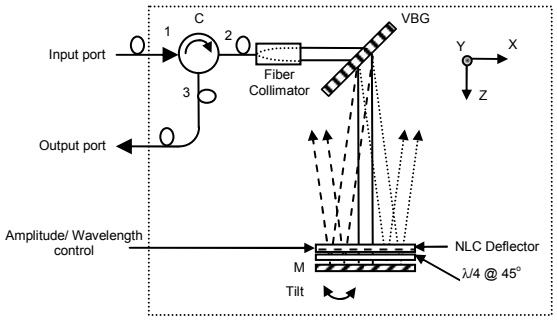

Fig. 4. Proposed Wavelength Tunable Variable Fiber-Optic Attenuator Using Liquid Crystal-Mirror Hybrid Controls. C: Optical Circulator; VBG: Volume Bragg Grating; M: Mirror.

operations so that the polarization dependent LC deflectors operate as polarization independent devices. The distance *d* between M and the GRIN lens is such that the Gaussian beam emerging from the GRIN lens forms its minimum beam waist at the mirror location leading to a low loss self-imaging design.[16] The VBG is placed at the Bragg angle orientation θ_{Bragg} for the band central wavelength so that the input broadband source spectrum in the first order spreads by an angle of $2\Delta\theta = \theta_{max} - \theta_{min}$ along x-axis (see Fig. 4), all with the minimal insertion loss, where $\theta_{max}=\sin^{-1}[(\lambda_{max}/L)-\sin\theta_{Bragg}]$ and $\theta_{min}=\sin^{-1}[(\lambda_{min}/L)-\sin\theta_{Bragg}]$, and L is the grating period. For the designed VOA operating spectrum, λ_{max} and λ_{min} correspond to the maximum and minimum wavelength values, respectively. An anti-parallel rub nematic LC (NLC) deflector is placed adjacent to M. Mirror M is a one dimensional tilt mirror used for selection of wavelength. If mirror based two dimensional x-y steering is deployed for both coarse wavelength selection and attenuation, two independent mirrors should be used to avoid crosstalk. The output of the module is always the chosen narrow band of the input light that is Bragg coupled back via the VBG into the GRIN lens. The extent of this narrow band $\Delta\lambda$ is defined by the VBG resolution and is expressed as $\Delta\lambda = \frac{L\lambda}{|m|W}$, where m is the grating order number, λ is the hybrid LC-mirror optics selected Bragg wavelength, and W is the $1/e^2$ beam diameter incident on the grating.[24] Due to the divergent nature of the beam produced by the VBG, only the Bragg matched component of the light is coupled back into the GRIN lens and hence enters the SMF. The rest of the off-axis unselected input light after double pass through the VBG does not enter the SMF. For selecting the desired wavelength to be coupled back into the GRIN lens, first the mirror M is tilted about the *y*-axis in order to select the correct Bragg angle for the chosen wavelength within the source spectrum. M can provide a wide tilt angle range needed to cover a broad spectral/angular band of the input light signal, although with limited mirror fine positioning repeatability. This fine tilt tuning need can be handled by using another NLC deflector in the module that is driven by a given voltage signal that accurately fine tweaks the beam deflection angle about *y*-axis to match the desired Bragg angle for the chosen wavelength. Once the wavelength is chosen, the next step is the VOA implementation for this given wavelength. This is achieved via the NLC deflector based beam deflection

about *x*-axis. Fundamentally here, attenuation is realized via returning beam misalignment along the *y*-direction (not the grating vector direction) into the GRIN lens.[16] Thus, the hybrid LC-mirror controls give both high dynamic range and high resolution for controls of the proposed module.

LC-Deflector Based Wavelength Tunable VOA Experiment

For the proof-of-concept experiment, the Fig. 4 design is implemented in the laboratory. The SMF GRIN lens used has a 5 mm physical diameter with a 2.5 mm exit beam $1/e^2$ diameter. The beam waist location distance *d* of the chosen GRIN lens is 25 cm and the $1/e^2$ beam diameter at beam waist location is 2.49 mm. The QWP positioned within 2 mm of the mirror is oriented at 45° with respect to the NLC director.

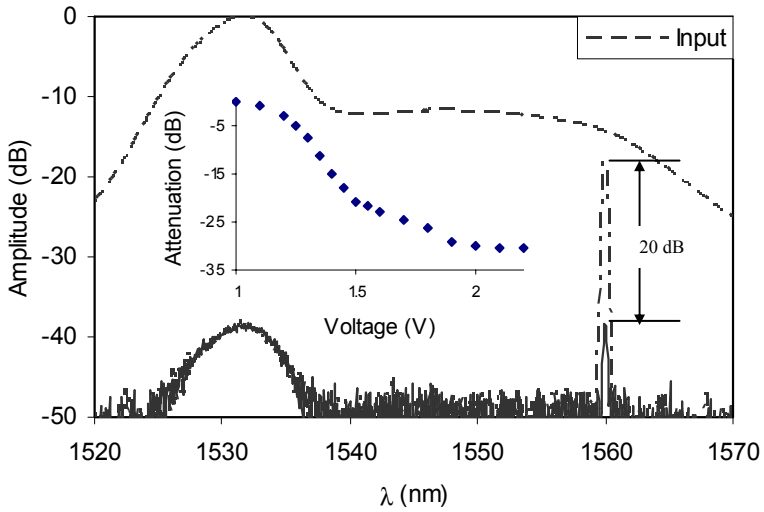

Fig. 5. Proposed Wavelength Tunable Variable Fiber-Optic Attenuator operating as VOA for mirror M selected wavelength of 1560 nm and attenuation plots for 0 and 20 dB settings using NLC deflector driven at two different operating voltages. (Inset) Module operating as a VOA for the mirror M direction selected 1550 nm wavelength.

The distance between the NLC deflector and the QWP is 9.5 mm. The total fiber-to-fiber module insertion loss measured is 3.7 dB which includes a 0.7 dB loss per pass through the non-AR coated NLC deflector, a 0.1 dB insertion loss for the freespace-to-fiber distance between the NLC deflector and the QWP is 9.5 mm. The total fiber-to-fiber module insertion loss measured is 3.7 dB which includes a 0.7 dB loss per pass through coupling via the self-imaging mechanism, a 1.4 dB circulator loss, and 0.4 dB loss per pass through the VBG. Insertion loss variation for the module was measured to be ±0.2 dB in the entire 1520-1570 nm band.

Amplified spontaneous emission (ASE) from an erbium doped fiber amplifier was used as the broadband input source for the wavelength agile VOA. The VBG placed 4 cm away from the GRIN lens is a 980 lines/mm Dickson grating that spreads the 50 nm source spectrum by 4.55° which corresponds to a linear spread of 1.67 cm at the mirror M. The grating Bragg center wavelength λ_{Bragg} chosen is 1550 nm and θ_{Bragg} is 46.76°.

Figure 5 (dashed line) shows Optical Spectrum Analyzer (OSA) traces of the input source spectrum from 1520 nm to 1570 nm wavelength range. The VBG resolution $\Delta\lambda$ is calculated to be 0.27 nm which is verified by the measured FWHM bandwidth of the module output light spectra as seen in Fig. 5. The NLC deflector used has a diameter of 5 mm and a NLC layer with a uniform thickness of 50 μm.[19] The NLC deflector is oriented to perform fine VOA operations by deflecting the beam about x-axis with M set initially for the 1550 nm test wavelength that enables retro-reflection via the entire optics. To demonstrate the broadband operation of the module as a wavelength selective VOA, the mirror M is tilted about the y-axis to set the reflection at 1560 nm as shown in Fig. 5, with attenuation controlled via NLC deflector drive controls. The selected spectrum shows two attenuation settings of 0 dB and 20 dB. Note that the present wavelength tuning performance depends upon the characteristics of the mechanical mirror stage used, in this case a standard commercial Newport stage. In general, note that any small variation of this or any other stage over a long period of time can be compensated for using the NLC deflector based wavelength tuning, an additional feature of the proposed module. Module PDL is measured to be < 0.1 dB over the entire 1520-1570 nm wavelength band. The fine attenuation control resolution of the NLC deflector is measured to be 0.05 dB for a chosen 1550 nm wavelength with an attenuation dynamic range of 30.6 dB by changing the drive voltage to the NLC deflector as also shown in the Fig. 5 inset.

To demonstrate fine precision no moving parts wavelength selection in the module, the Fig. 4 NLC deflector is engaged. To perform this experiment, the NLC deflector in the previous setup is rotated by 90^{o} in order to produce the needed fine beam deflection about *y*-axis. Since the NLC deflector has a metallic contact on each edge, the electric field gradient formed is either in $+x$ direction or in $-x$ direction. This leads to the capability of tuning the wavelength twice that of a deflector with a single electrical contact. When the drive signal is applied in order to cause a voltage gradient in the $+x$ direction the optical beam gets deflected in the $+x$ direction and as a result a slightly different wavelength is coupled back to the GRIN lens. The total wavelength fine tunability that was experimentally achieved by using the two aforementioned electrical contacts in order to get deflection in both $+x$ and $-x$ direction was measured to be 1.44 nm with a drive signal of 2.2 V_{pp} as shown in Fig. 6. Assuming that the VBG resolution is not a limiting factor, the optical spectrum analyzer measured NLC deflector wavelength tuning resolution is 10±2 pm. The solid curve in Fig. 6 corresponds to no applied signal while the two dashed curves correspond to 2.2 V_{pp} applied signal at 1 KHz square waveform to the two opposing linear metallic contacts, resulting in a FWHM spectral width of 0.29 nm, 0.27 nm and 0.29 nm (viewing Fig. 6 from left to right).

Response Time

A key VOA parameter is its longest reset time. $t_s=t_1+t_2$ where t_1 is the NLC response time to set the NLC deflector to a given required beam steering voltage V. t_2 is the NLC deflector response time when V=0 and the device is reset to its zero beam steering angle state. For a homogeneous NLC cell the response time is given by:[23]

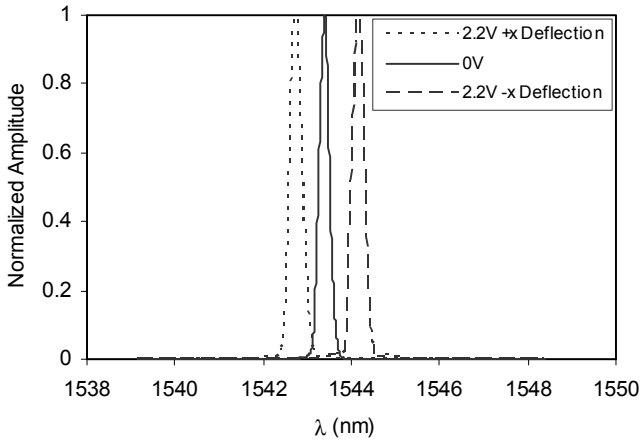

Fig. 6. Proposed Wavelength Tunable Variable Fiber-Optic Attenuator operating with precise fine wavelength selection using NLC deflector driven at three different operating states giving a 1.44 nm liquid crystal tuned fine wavelength range.

$$\tau_r = \frac{\tau_o}{\left| \left(\frac{V}{V_{th}} \right)^2 - 1 \right|}, \tag{16}$$

where τ_o is the LC director's relaxation time and is given as:[18]

$$\tau_o = \frac{\gamma_1 t^2}{\pi^2 K_{11}}, \tag{17}$$

and V_{th} is the NLC threshold voltage and is given by:[23]

$$V_{th} = \pi \sqrt{\frac{K_{11}}{\varepsilon_o \Delta\varepsilon}}, \tag{18}$$

where K_{11} is the splay elastic constant, ε_o is the free-space dielectric permittivity, $\Delta\varepsilon$ is the dielectric anisotropy, and γ_1 is the visco-elastic coefficient. As can be noted from the equations (16-18), V_{th} is more or less constant for a certain NLC and τ_o depends on the cell thickness t. For a given cell size and NLC material, τ_o will be fixed and hence the response time τ_r depends only on the ratio V/V_{th}. The response time decreases as the ratio V/V_{th} is increased. For the present VOA, its longest reset time t_s can be approximated by using $t_1=\tau_r$ and $t_2=\tau_o$. Hence the VOA maximum reset time is

$$t_s = \tau_r + \tau_o . \tag{19}$$

Since τ_o is generally fixed, it can be concluded from equation (19) that the VOA reset time is not the same for the different attenuation levels. For example, to reset the VOA for maximum attenuation, the reset time is the shortest as $V>>V_{th}$.

Notice from equation (17) that the NLC deflector device response time τ_o has a square law relation with the NLC cell thickness t; hence a reduction in the cell thickness will result in a shorter overall reset time for the VOA. For example, reducing the thickness by half will result in a 4 times faster VOA response. Recall that the NLC deflector used is a non-pixelated NLC cell making the device refractive in nature as

opposed to a diffractive device that would otherwise give unwanted diffraction orders and hence excess loss.

The NLC used has a large nematic temperature range from -15°C to 113°C.[25] In a typical NLC material, birefringence decreases as a function of temperature. In an NLC based VOA where BDPs are used to separate and recollect the orthogonal polarized light components, temperature change causes birefringence change leading to polarization extinction ratio changes. This causes the light throughput fluctuations in the VOA that can cause irrecoverable light loss. Due to the beam steering nature of the proposed NLC-based VOA, a temperature change causes a birefringence change in the NLC deflector leading to a change in deflection angle and hence attenuation level. More importantly, the desired VOA attenuator level can be recovered by electrically controlling the NLC deflector to recover the original deflection angle. Unlike the BDP-based LC VOAs, the NLC deflector based VOA does not suffer from irrecoverable VOA excess loss. Specifically, the proposed VOA when used with a feedback loop can operate properly even in an environment with temperature swings and no temperature stabilization hardware. Reset speed of the module is linked to the speed of mirror-control and NLCs that have typical response times of the order of a few milliseconds. Response time of the NLC cell used is ~1 second due to its relatively large thickness compared to ordinary NLC devices. Multiple thin NLC cells each giving an incremental value of the total deflection angle and a typical low 0.04 dB loss, can be cascaded in order to achieve the desired attenuation and wavelength control resolution and dynamic range with a relatively faster response time. Research is underway to synthesize NLC materials for larger birefringence and smaller viscosity in order to obtain faster response times.[25] Faster response times can also be achieved for NLCs using either the dual frequency effect or the transient-nematic effect.

Extended Applications

The VOA architectures shown in Figure 1 can be extended to other useful devices. Specifically, a 1x2 switch is formed by replacing the output port single fiber collimator in Figure 1(a) by a dual fiber collimator and inserting a half wave plate in-between the two NLC deflectors that have their directors parallel to each other (see Figure 7(a)). The half wave plate is present so that both the polarization components are steered into the same direction. For such a 1x2 switch, the insertion loss is estimated to be <0.67 dB using AR coated devices. This 0.67 dB mainly comes from the absorption in the NLC material and can be reduced by having a thinner NLC layer and smaller device aperture. Also notice that the two NLC deflectors can be driven individually so as to cancel the effects of thickness variation in different cells or to get an even finer control over the device operation. Figure 7(b) shows an alternate structure for the 1x2 switch using a triple fiber collimator in a reflective design. Such a programmable compact 1x2 switch can be useful in photonic applications where on-demand programmable signal taps are needed for in line spectral analysis and power monitoring.

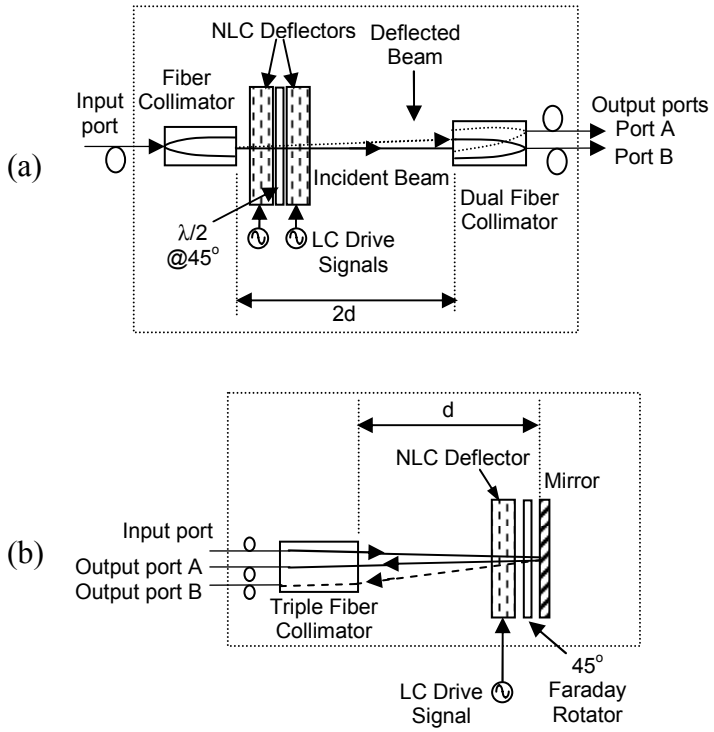

Fig. 7. Proposed NLC deflector based 1x2 switch designs using (a) a single fiber collimator, two parallel aligned NLC deflectors, a half wave plate and a dual fiber collimator, and (b) a triple fiber collimator and a single NLC deflector in a reflective mode.

Conclusion

The power of combined LC-mirror optics approach is shown for enabling a wavelength selective VOA module. The LC optics are used for fine beam steering while the mirror optic is engaged for larger angle beam steering within the fiber-optic module, thus playing into the strengths of the two steering technologies. A proof-of-concept module is designed and indeed demonstrates the wide dynamic range as well as high resolution capabilities for both wavelength selection and light attenuation controls. Improvements in the attenuation coarse dynamic range of the module is possible using a non-circulator based two fiber module design. In summary, novel fiber-optic VOA architectures are demonstrated using an electrically controlled NLC deflector that implements optical power attenuation via beam spoiling-based single-mode fiber coupling loss. The proposed VOA can be electrically compensated to deliver a fixed excess loss with changing environmental conditions. The VOA features a compact no moving parts design with high attenuation dynamic range, low loss, low PDL potential, and fine wavelength selectivity in a broad optical wavelength band. Experiments demonstrate fiber-optic component specifications useful for many applications, such as for test instrumentation and fiber-optic communications. The basic VOA design can also be extended to realize a small 1x2 switch.

References

1. C. Marxer, P. Griss, N. de Rooij, "A variable optical attenuator based on silicon micromechanics," IEEE Photonics Technology Letters, Vol. 11, Issue 2 , Pages 233-235, February 1999.
2. M.J. Mughal and N. A. Riza, "Compact acoustooptic high-speed variable attenuator for high-power applications," IEEE Photonics Technology Letters, Vol. 14, Issue 4, Pages 510-512, April 2002.
3. X. Orignac, "First ion-exchanged dual thermo-optic variable optical attenuator," International Conference on Transparent Optical Networks, Pages 89-92, 9-11 June 1999.
4. J. L. Jackel, J. J. Veselka, and S. P. Lyman, "Thermally tuned glass Mach-Zehnder interferometer used as a polarization insensitive attenuator," Applied Optics, Vol. 24, No. 5, Pages 612-614, March 1985.
5. R. A. Soref, "Liquid-crystal fiber-optic switch," Optics Letters, Vol. 4, Issue 5, Pages 155-157, May 1979.
6. E. G. Hanson, "Polarization-independent liquid-crystal optical attenuator for fiber-optics applications," Applied Optics, Vol. 21, Issue 7, Pages 1342-1344, April 1982.
7. K. Hirabayashi, M. Wada and C. Amano, "Compact Optical-Fiber Variable Attenuator Arrays with Polymer-Network Liquid Crystals," Applied Optics-LP, Vol. 40, Issue 21 Pages 3509-3517, July 2001.
8. J. J. Pan, H. Wu, W. Wang, X. Qiu and J. Jiang, "Temperature independent, accurate LC VOA through electric feedback control," Proceedings of National Fiber Optics Engineers Conference (NFOEC), Pages 943-949, Orlando, Florida, USA, September 2003.
9. N. A. Riza, "Fault-tolerant fiber-optical beam control modules," US Patent No. 6,222,954, April 24, 2001.
10. N. A. Riza and Y. Huang, "Digital fault-tolerant variable fiber optic attenuator using liquid crystals," Advances in Optical Information Processing IX, Proc. SPIE Vol. 4046, Pages 101-106, Dennis R. Pape; Ed., July 2000.
11. N. A. Riza, "Multi-technology multi-beam-former platform for robust fiber-optical beam control modules," US Patent No. 6,525,863, February 25, 2003.
12. N. A. Riza and S. Khan, "Liquid-Crystal-Deflector Based Variable Fiber-Optic Attenuator," Applied Optics, Vol. 43, Issue 17, Page 3449-3455, June 2004.
13. N. A. Riza and S. A. Khan, "Wavelength Tunable Variable Fiber-Optic Attenuator Using Liquid Crystal-Mirror Hybrid Controls," IEEE Photonics Technology Letters, Vol. 17, Issue 3, Page 621-623, March 2005.
14. K. Nakamura, T. Saitoh and Y. Takahashi, "High-speed optical performance monitor for WDM network using MEMS scanning mirror," IEEE/LEOS International Conference on Optical MEMS, Pages 97-98, Waikoloa, Hawaii, August 2003.
15. J. Berger, F. Ilkov, D. King, A. Tselikov, D. Anthon, "Widely tunable, narrow optical bandpass Gaussian filter using a silicon microactuator," Optical Fiber Communication Conference, 252-253, Atlanta, GA, 23-28 March 2003.
16. M. van Buren and N. A. Riza, "Foundations for Low-Loss Fiber Gradient-Index Lens Pair Coupling with the Self-Imaging Mechanism," Applied Optics-LP, Vol. 42, Issue 3, Pages 550-565, January 2003.
17. S. Yuan, and N. A. Riza, "General Formula for Coupling-Loss Characterization of Single-Mode Fiber Collimators by use of Gradient-Index Rod Lenses," Applied Optics-LP, Vol. 38, Issue 15, Pages 3214-3222, May 1999.
18. G. D. Love, J. V. Major and A. Purvis, "Liquid-crystal prisms for tip-tilt adaptive optics," Optics Letters, Vol. 19, Issue 15, Pages 1170-1172, August 1994.
19. A. F. Naumov, M. Yu. Loktev, I. R. Guralnik, and G. Vdovin, "Liquid-crystal adaptive lenses with modal control," Optics Letters, Vol. 23, Issue 13, Pages 992-994, July 1998.
20. L. M. Blinov, Electro-optical and magneto-optical properties of liquid crystals (John Wiley & Sons Ltd., Chichester, U.K., 1983).
21. Merck Liquid Crystals Catalog, Darmstadt, Germany, 2003.
22. S. T. Wu, School of Optics and the Center for Research and Education in Optics and Lasers, University of Central Florida, 4000 Central Florida Blvd., Orlando, FL 32816-2700 (Personal communication, 2003).
23. I. C. Khoo and S. T. Wu, Optics and nonlinear optics of liquid crystals (World Scientific, Singapore, 1993).

24. Z. Yaqoob and N. Riza, "Low-loss wavelength-multiplexed optical scanners using volume Bragg gratings for transmit-receive lasercom systems," Optical Engineering, Vol. 43, Issue 5, Pages 1128-1135, May 2004.
25. S. Gauza, H. Wang, C. Wen, S. Wu, A. Seed, and R. Dabrowski, "High Birefringence Isothiocyanato Tolane Liquid Crystals," Japanese Journal of Applied Physics Part I, 42, 3463-3466, 2003.

Table 1

VOA Design Parameters			Fiber-optic Coupling Beam Spoiling Parameters		
t (μm)	D (mm)	d (cm)	θ_w (mrad)	θ_e (mrad)	x_o (mm)
10	0.42	2	23.81	38.82	0.78
10	0.4	4	25	40.76	1.63
20	0.42	2	47.64	77.7	1.56
20	0.4	4	50	81.59	3.27
50	0.42	2	119.33	195.29	3.96
50 *	5 *	25 *	2.29	3.73	0.93

Table 1: VOA Design Parameters v.s. Obtained Beam Spoiling Parameters. t: NLC deflector cell thickness; D: NLC deflector cell aperture; d: GRIN lens beam waist distance from GRIN lens exit aperture, θ_w: NLC deflector maximum deflection angle, θ_e: maximum freespace exit angle from the NLC deflector, and x_o: maximum offset error due to angular deflection.
*Demonstrated experimental design.